Journal of Power Sources 242 (2013) 631–637

Contents lists available at SciVerse ScienceDirect

Journal of Power Sources

journal homepage: www.elsevier.com/locate/jpowsour

A novel electroless method to prepare a platinum electrocatalyst on diamond for fuel cell applications

Xiao Lyu [a,b], Jingping Hu [a,*], John S. Foord [a,*], Qiang Wang [c]

[a] Chemistry Research Laboratory, Department of Chemistry, University of Oxford, Mansfield Rd, Oxford OX1 3TA, United Kingdom
[b] School of Materials Science and Engineering, Shenyang Ligong University, No.6 Nanping Central Rd, Shenyang 110159, PR China
[c] Key Laboratory of Electromagnetic Processing of Materials, Northeastern University, No.3 Wenhua Rd, Shenyang 110819, PR China

HIGHLIGHTS

- A novel route to prepare dispersed Pt nanoparticles on conductive diamond supports is identified.
- The method uses a combination of electroless and electrolytic reactions.
- Highly dispersed, adherent Pt nanoparticles are distributed evenly over the support.
- A significant advance towards diamond supported catalysts for fuel cell application is achieved.

GRAPHICAL ABSTRACT

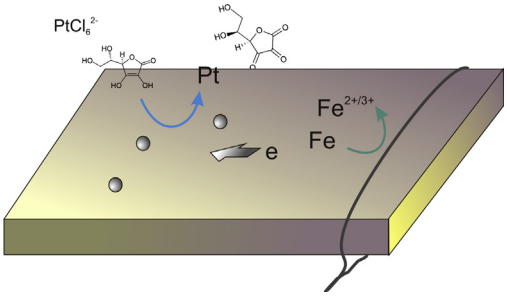

ARTICLE INFO

Article history:
Received 18 December 2012
Received in revised form
13 May 2013
Accepted 14 May 2013
Available online 6 June 2013

Keywords:
Platinum
Diamond
Electroless
Ascorbic acid
Methanol oxidation
Fuel cell

ABSTRACT

A novel electroless deposition method was demonstrated to prepare a platinum electrocatalyst on boron doped diamond (BDD) substrates without the need for pre-activation. This green method addresses the uniformity and particle size issues associated with electrodeposition and circumvents the pre-activation procedure which is necessary for conventional electroless deposition. The inert BDD substrate formed a galvanic couple with an iron wire, to overcome the activation barrier associated with conventional electroless deposition on diamond, leading to the formation of Pt nanoparticles on the electrode surface in a galvanic process coupled to a chemical process. When sodium hypophosphite was employed as the reducing agent to drive the electroless reaction Pt deposits which were contaminated with iron and phosphorus resulted. In contrast, the reducing agent ascorbic acid gave rise to high purity Pt nanoparticles. Optimal deposition conditions with respect to bath temperature, pH value and stabilizing additives are identified. Using this approach, high purity and uniformly distributed platinum nanoparticles are obtained on the diamond electrode surface, which demonstrate a high electrochemical activity towards methanol oxidation.

1. Introduction

Proton exchange membrane fuel cells (PEMFCs) are promising alternatives to the present power sources due to their high operational efficiencies and environmentally benign working characteristics. The wide application of PEMFCs is limited by the cost of electrocatalysts, typically platinum and platinum alloys [1]. Optimized performance and cost control of these electrocatalysts requires a large electroactive area, smaller particle size and a high stability against agglomeration or catalyst loss from the electrode surface.

Various carbon materials have been extensively investigated for their potential usage as electrocatalyst supports in fuel cells, such as

* Corresponding authors. Tel.: +44 1865 275967; fax: +44 1865 275410.
E-mail addresses: jingping.hu@chem.ox.ac.uk (J. Hu), john.foord@chem.ox.ac.uk (J.S. Foord).

0378-7753/$ – see front matter © 2013 Elsevier B.V. All rights reserved.
http://dx.doi.org/10.1016/j.jpowsour.2013.05.057

graphite, glassy carbon, carbon nanotubes and carbon nanofibers [2–5]. These electrodes are limited by the stability of the sp^2-bonded carbon support materials, for example loss of active Pt has been reported as a result of electrocorrosion of the support [6,7]. Interest has begun to develop more recently in the use of conductive boron-doped diamond (BDD) as an alternative support [8–21]. Compared to other carbon materials, BDD possesses outstanding properties as an electrocatalyst support, such as a long-term thermal stability without surface oxidation, an extreme chemical stability and corrosion resistance in a hostile environment [22,23]. This material is now routinely available at a relatively cheap cost grown by chemical vapour deposition, including in small nanoparticle form for the preparation of porous electrodes [15–20].

Numerous approaches have been reported for the deposition of Pt and other metal nanoparticles on BDD substrates for fuel cell electrocatalysts. Wet impregnation is not an ideal route for BDD due to the weak adsorption of metal ions on diamond surfaces. Sol gel [10,13] and microemulsion [8,9] can produce electrocatalysts of high activity on diamond but problems with the control of particle size and distribution still exist [14], and the stability is poor due to low adhesion of pre-formed metal nanoparticles on diamond. Electrodeposition provides a better way to produce adherent particles [19,24,25], but the deposition is not sufficiently uniform, especially for BDD substrates with a heterogeneous electroactivity attributable to the non-uniform boron doping in diamond crystals [26–28]. Electroless deposition (ED) is another widely used method for electrocatalyst deposition [29,30]. In this method, metallic electrocatalysts are deposited, using solutions containing reducing agents and metal ion precursors, onto specific sites of a catalytic surface which can either be an active substrate or an inert substrate seeded with a catalytically active metal. For the ED of Pt, it is essential for the BDD substrate to undergo sensitization and activation pretreatment [31], by coating with a thin layer of catalyst such as nickel or tin. However this is undesirable for the present application since these elements will interfere with the catalytic activity of the platinum and complicate the manufacturing process. To tackle this issue, we demonstrate, for the first time, a novel method to electrolessly deposit Pt on inert electrodes without the need for pre-activation.

In this new method, an iron electrode was contacted to the diamond substrate to form a galvanic couple in the electroless plating bath, and it is shown platinum nanoparticles are successfully deposited on the inert diamond substrate using this approach. Although ED of iron alloys on Cu substrates by contacting with an Al strip has been reported [32], this paper is the first to explore this method for ED of fuel cell electrocatalysts on an inert substrate. The use of sodium hypophosphite and ascorbic acid as reducing agents was compared, and the deposition process was controlled by adjusting bath temperature, pH value and addition of stabilizers. This novel ED approach was demonstrated to form highly active, uniformly distributed and stable Pt electrocatalysts for fuel cell application without a pre-activation process.

2. Experimental

Boron doped diamond wafers ([B] $>$ 10^{20} cm^{-3}) of $10 \times 10 \times 0.6$ mm were purchased from Element Six Co. Iron wire (99.5%) of 0.2 mm diameter was from Advent Research Materials Ltd. Dihydrogen hexachloroplatinate (IV) hexahydrate (99.9%) ($HPtCl_6 \cdot 6H_2O$) was purchased from Alfa Aesar. Sodium hypophosphite monohydrate ($NaH_2PO_2 \cdot H_2O$, 99.0%), L-Ascorbic acid ($C_6H_8O_6$, 99.0%), sodium citrate ($C_6H_5O_7Na_3 \cdot 2H_2O$) and hexadecyltrimethylammonium bromide (CTAB, 99%) were obtained from Sigma–Aldrich. All solutions were prepared using milli-Q water ($>$18 MΩ cm).

During ED, a BDD wafer in contact with a 10 mm iron wire was immersed in the plating solution and served as a support substrate. When sodium hypophosphite was employed as a reducing agent, the composition of precursor solution was: 50 mM H_2PtCl_6, 300 mM sodium hypophosphite, and 34 mM sodium citrate as a complexing agent to stabilize platinum ions. When ascorbic acid was used as a reducing agent, the precursor solution was composed of 5 mM H_2PtCl_6, 10 mM ascorbic acid and 3 mM sodium citrate, and the pH value was adjusted to 4 using NaOH.

Electrochemical experiments were performed at room temperature using a CHI900B electrochemical workstation (CH Instrument), with a platinum counter electrode and a Ag/AgCl reference electrode against which all electrode potentials in this paper are quoted. The BDD working electrodes were mounted in a home-built PTFE holder with a circular area of 0.317 cm^2 exposed to the electrolyte. The morphology was characterised by SEM (JEOL JSM-6500F) and AFM in tapping mode (Veeco NanoScope). XPS characterisation was conducted using an Al Kα (1486.6 eV) X-ray source and hemispherical electron energy analyser. UV spectra were recorded between 200 and 400 nm using a Lambda 750S UV/Vis spectrophotometer to estimate platinum loading.

3. Results and discussion

3.1. Electroless deposition using sodium hypophosphite as the reducing agent

Electroless deposition was initially conducted using sodium hypophosphite as a reducing agent in the absence of an iron wire, but no deposition was observed, which is expected as a substrate sensitization and activation pretreatment is routinely required for inert substrates [30,31]. Therefore we explored the use of an iron wire in electroless deposition. After placing an iron wire in contact with the BDD substrate in sodium hypophosphite containing precursor bath, platinum nanoparticles were electrolessly deposited on the inert BDD. The presence of both iron wire and reducing agent was found essential to initiate the deposition.

The mechanism of this novel electroless deposition is proposed to be a combination of a galvanic process and a chemical reduction process. It was essential to keep the inert substrate connected with the iron wire in the plating solution, as no deposition was observed in the absence of iron wire or if the iron wire was not immersed in the solution or separated from the substrate in the presence of either reducing agent. In a galvanic process, we propose the iron wire acts as an anode; when iron undergoes oxidative dissolution, electrons are transferred to the BDD surface and platinum anions are reduced and deposited. The galvanic cell is described using the following notation:

$$Fe_{(s)} \left| Fe^{3+}_{(aq)} \right\| PtCl^{2-}_{6(aq)} \left| Pt_{(s)}, \quad E^{\Theta} = 0.778\ V \right.$$

It is stressed satisfactory results could not be observed using the Fe wire alone so a coupling between the galvanic process and the electroless chemical reduction process using reducing agents such as sodium hypophosphite or ascorbic acid is essential to obtain uniform and well controlled deposition.

The chemical composition of platinum containing deposits from ED in pH 11 solution at 65 °C was studied by XPS as shown in Fig. 1. The presence of platinum, iron and phosphorus on the BDD surface was confirmed from the survey spectrum (Fig. 1a). In high resolution scans, the Pt 4f peaks can be fitted to an elemental Pt $4f_{7/2}$ peak at 71.2 eV, an overlapping of the Pt oxide $4f_{7/2}$ peak and the elemental Pt $4f_{5/2}$ peak at 74.3 eV, and a Pt oxide $4f_{5/2}$ peak at 77.3 eV respectively, as shown in Fig. 1b, confirming the co-

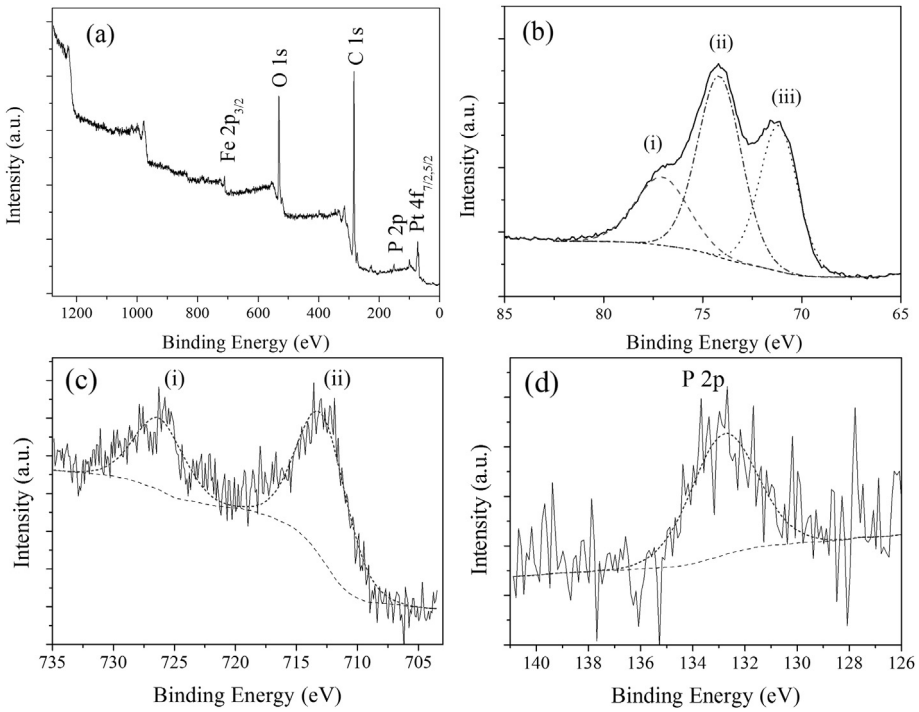

Fig. 1. XPS spectrum of platinum deposited on BDD in a bath of pH 11 at 65 °C for 10 min: (a) survey, (b) Pt 4f, (c) Fe 2p and (d) P 2p spectrum. (b) (i) Pt $4f_{5/2}$ (oxide), (ii) mixture of Pt $4f_{7/2}$ (oxide) and $4f_{5/2}$ (elemental), (iii) $4f_{7/2}$ (elemental). (c) (i) Fe $2p_{1/2}$ and (ii) Fe $2p_{3/2}$.

deposition of platinum in mixed elemental and oxide form [33,34]. The binding energy of the elemental Pt $4f_{7/2}$ peak is slightly higher than the typical value (70.9 eV) in the literature [35], suggesting Pt alloying with iron and phosphorus, similar to the case of other Pt alloys in a more electropositive environment such as Pt–Sn and Pt–Ge [36,37]. An Fe $2p_{3/2}$ peak was observed at around 712.8 eV (Fig. 1c), suggesting most iron is in the Fe^{3+} state [35,38,39]. A broad P 2p peak appears between 131 and 134 eV, and is attributable to phosphorus oxides, such as phosphite, phosphate and pyrophosphate [40,41]. The co-deposition of phosphorus is typical in electroless deposition when hypophosphite is used as a reducing agent [30], due to a side reaction:

$$2H_2PO_2^- + 2H_2O \rightarrow 2HPO_3^- + 4H^+ + 2H_{ads} + 2e^-$$

$$H_{ads} + H_2PO_2^- \rightarrow P + OH^- + H_2O$$

The results confirm that a chemical reduction process coupled with a galvanic process initiated by the reduction of iron wire can be used to deposit Pt on inert substrates such as diamond, but under these initial conditions the deposits produced are impure.

The influence of pH and temperature during deposition on film composition was also quantified by XPS analysis. The relative atomic concentrations at various deposition conditions were calculated using atomic sensitivity factors [42], as shown in Table 1. The C and O signals largely arise from the diamond substrate, but the Fe, Pt and P components clearly arise from deposition. The Pt content of the deposited electrocatalysts was found to be relatively insensitive to temperature in contrast to the change of P content which rose rapidly at higher temperature. This suggests that iron is deposited from the electrochemical process while phosphorus originates from the chemical process which is much more temperature sensitive than the former. With an increasing pH value, an increase of both the platinum and iron deposition rates increase, whilst a decrease of P content was observed, suggesting high pH values are preferred to minimise P contamination.

The electrochemical properties of platinum deposits on BDD were characterized by cyclic voltammetry in 0.5 M H_2SO_4 as shown in Fig. 2a and b. Since the P content can be minimised and Pt loading can be maximised at higher pH and lower temperature, Pt deposition from a basic bath (pH 11) at 65 °C was employed. The most obvious features are the reduction peak at around 0.4 V which can be attributed to the reduction of platinum oxide to metallic platinum [43], and the oxidation peak at around −0.05 to −0.15 V which is associated with oxidative hydrogen desorption from the platinum surface [17,44]. As anticipated from the XPS data these Pt-induced features increase at higher temperatures. The hydrogen desorption peak can be used to estimate the electrochemical active surface (EAS, $m^2\ g^{-1}$) of platinum:

$$EAS = 0.1\frac{Q_H}{[Pt] \times 0.21}$$

where Q_H is the hydrogen desorption charge ($mC\ cm^{-2}$), [Pt] is the platinum loading ($mg\ cm^{-2}$) on BDD and 0.21 ($mC\ cm^{-2}$) represents the charge required to oxidize a monolayer of hydrogen on a

Table 1
Composition of deposits prepared at different deposition conditions for 10 min.

Composition (%)	Temperature (°C) (pH 11)			pH value (65 °C)		
	55	65	75	3	7	11
C	78.30	77.44	76.05	81.24	79.51	77.44
O	19.75	20.43	21.17	17.75	19.04	20.43
Pt	1.54[a]	1.53[a]	1.34	0.47	1.02	1.53[a]
Fe[b]	0.31	0.38	0.27	0.10	0.19	0.38
P	0.094	0.22	1.18	0.44	0.24	0.22

[a] Part of platinum exists in the form of oxide.
[b] Iron exists in the form of oxide.

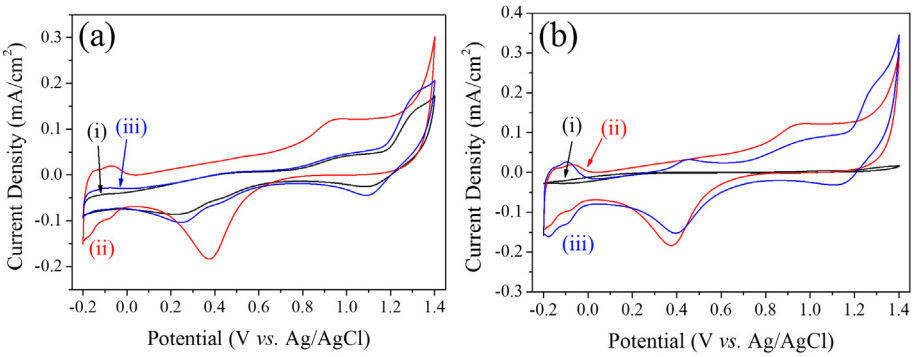

Fig. 2. Cyclic voltammograms of platinum deposited on smooth BDD normalized to the geometry area of electrode in a bath at (a) various temperatures at pH 11: (i) 75 °C, (ii) 65 °C, (iii) 55 °C; (b) at various pH at 65 °C: (i) pH = 3, (ii) pH = 11, (iii) pH = 7 for 30 min (except for 10 min at 75 °C).

Pt (111) surface [45,46]. Q_H is calculated to be around 0.087 mC cm^{-2} from the voltammograms. The Pt loading can be estimated from AFM and SEM imaging of the Pt covered surface. The AFM image in Fig. 3a shows a typical particle diameter of around 50 nm. The morphology was also examined by SEM, as presented in Fig. 3b, showing platinum nanoparticles of around 30–50 nm diameter well dispersed on the diamond surface assuming a hemisphere geometry and using the particle size and density from AFM and SEM images shown in Fig. 3 Based on these data, the specific EAS value is estimated to be around 3.9 m^2 g^{-1}. This is consistent with an area of about 3 m^2 g^{-1} calculated from the AFM and SEM images assuming the hemispherical geometry. The dispersion observed is fairly similar for simple electrochemical deposition on diamond [47], however we demonstrate below even higher dispersions can be achieved by varying the deposition conditions.

3.2. Electroless Pt deposition using ascorbic acid as the reducing agent

Although the conventional pre-activation process in Pt electroless deposition can be circumvented, as shown above, by a coupled galvanic process with an iron wire on a BDD support, the co-deposition of phosphorus and iron raises a new problem since these elements will interfere with the catalytic activity of the Pt. Strong reducing agents such as hydrazine have been used to eliminate the co-deposition of other elements and achieve a high purity [48] but hydrazine is environmentally hazardous. The alternative use of ascorbic acid was therefore explored here; compared to sodium hypophosphite or hydrazine, ascorbic acid is cheap and environmentally friendly [49–51].

In the presence of ascorbic acid as a reducing agent, platinum nanoparticles were again deposited on the BDD substrate when in contact with an iron wire. It was critical to have both the iron wire and ascorbic acid present in order to have a satisfactory Pt deposition, as no platinum was observed in the absence of iron wire after deposition at 0 °C for 70 min, as shown in Fig. 6a(v). The purity of Pt deposits is confirmed by the XPS spectrum as shown in Fig. 4, where no trace of iron or phosphorus is discerned at least above the detection limit of the XPS technique. The high resolution spectrum shown in the inset exhibits a pair of strong peaks attributable to Pt $4f_{7/2}$ and Pt $4f_{5/2}$ at 71.4 and 74.7 eV respectively, implying that platinum is in the metallic state. The high purity metallic platinum nanoparticles from ascorbic acid reduction are obviously advantageous compared to the co-deposition of Pt, P and Fe from sodium hypophosphite reduction.

As ascorbic acid is quite a strong reducing agent, it was found the reduction reaction was so vigorous at room temperature that Pt aggregation quickly built up on more electroactive facets, as shown in SEM image in Fig. 5a. In addition, reduction of platinum inside the solution also commenced after 70 min as indicated by a change of solution colour.

To improve the uniformity, control the particle size and enhance the long term stability, various deposition conditions were explored, including addition of the surfactant CTAB, lowering of the bath temperature and ultrasonic substrate treatment in nanodiamond (ND, 3.5 nm) slurry. For a quantitative analysis of the platinum loading and catalytic performance, the mass of platinum

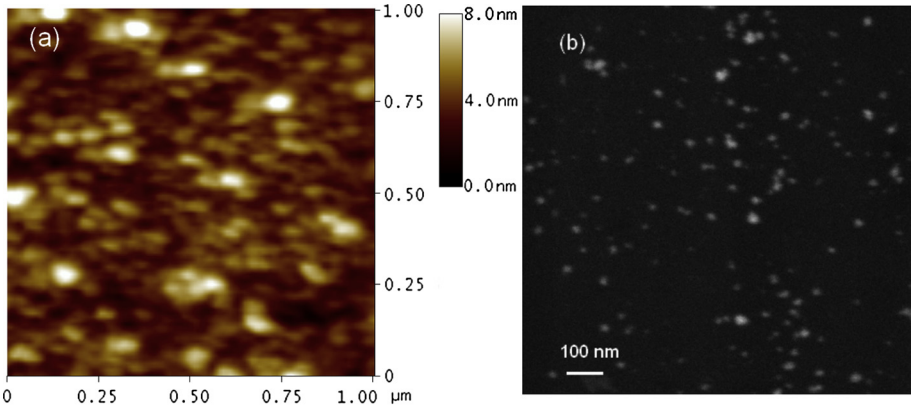

Fig. 3. (a) AFM image and (b) SEM image of Pt deposits on BDD prepared in a bath of pH 11 at 65 °C for 25 min.

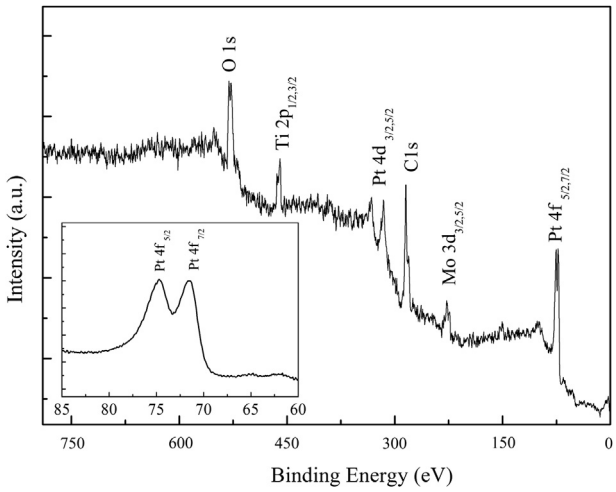

Fig. 4. XPS spectrum of platinum deposited on BDD using ascorbic acid as reducing agent at room temperature for 30 min, with spectrum for Pt $4f_{7/2}$ and $4f_{5/2}$ peaks in the inset.

was calculated from a spectrophotometric procedure by measuring the absorbance at 260 nm in the UV–Vis spectrum of the Pt complex in solution, in conjunction with a calibrated absorbance curve from known platinum concentration. From the calibration curve, the platinum loading was estimated to be around 72 μg cm^{-2} after the 70 min of deposition with addition of CTAB, in comparison to 163 μg cm^{-2} after 10 min of deposition without the presence of surfactant at room temperature. Addition of CTAB could greatly lower the reaction even at room temperature. The particle size was also greatly reduced, but aggregation of platinum particles still prevailed, as shown in SEM image in Fig. 5b. Compared to the use of surfactant, lowering the bath temperature is a more efficient method to optimize the distribution of Pt nanoparticles. A much more homogeneous and dense dispersion of platinum was observed in deposition at 0 °C, as shown Fig. 5c, with a platinum loading of 212 μg cm^{-2} after 70 min. In a previous publication, we found that ultrasonic treatment of BDD with non-catalytic nano- and microdiamond slurry can drastically improve the properties of deposits, such as dispersion, spatial uniformity, and stability [44]. The BDD electrode that underwent this pretreatment was used for electroless deposition at 0 °C, and a better uniformity and a much smaller particle size were observed, as shown in Fig. 5d.

The electrochemical performance of the electrocatalysts from electroless deposition at high Pt loadings as defined in Table 2 (up to 70 min. ED) was characterized by cyclic voltammetry, and the results are shown in Fig. 6. The hydrogen desorption peak in the voltammograms measured in sulphuric acid was used to estimate the EAS of platinum (Fig. 6a). Deposition at 0 °C without ultrasonic pretreatment shows the highest EAS value of 3.29 $m^2\ g^{-1}$, similar to EAS value of 2.25 for ultrasonic pretreated BDD, and in contrast to EAS values in the absence (of 2.82 $m^2\ g^{-1}$) and presence (1.51 $m^2\ g^{-1}$) of CTAB at room temperature (Table 2) due to the fast coalescence of platinum particles at high deposition rate and interaction with surfactant micelles. This EAS is in line with typical values for Pt electrodeposited on diamond [47]. Similar electroless deposition was also conducted on glassy carbon electrode, at 0 °C for 70 min, as shown in Fig. 6b. The glassy carbon with an iron wire connected during deposition shows platinum reduction and hydrogen desorption peaks clearly, indicating our novel deposition method can be applied to other similar inert electrodes.

The characteristics of methanol electrooxidation on platinum particles deposited on BDD under different conditions in 1.0 M

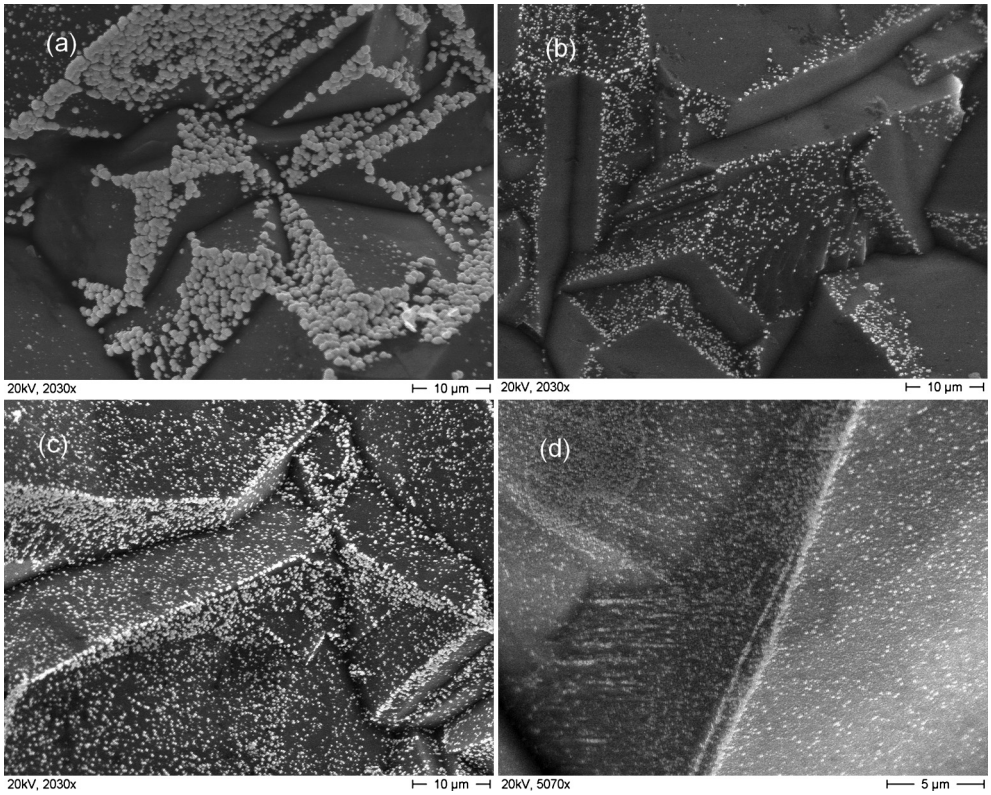

Fig. 5. SEM images of platinum electroless deposition under different conditions for 10 min: (a) room temperature, (b) room temperature and with CTAB in the plating bath, (c) at 0 °C and (d) at 0 °C on ultrasonic treated BDD.

Table 2
Electrochemical characterisation of Pt decorated BDD electrode prepared by electroless deposition, obtained from the hydrogen desorption in sulphuric acid or the forward scan of voltammogram peak in methanol.

Sample	Pt loading ($\mu g\ cm^{-2}$)	EAS ($m^2\ g^{-1}$)	Onset potential (V vs Ag/AgCl)	Mass activity ($A\ g^{-1}$)	Surface activity ($mA\ cm^{-2}$)
RT 10 min	163	2.82	0.305	0.45	0.13
RT CTAB 70 min	72	1.51	0.380	18.36	0.65
0 °C 70 min	212	3.29	0.297	3.32	0.42
0 °C ultrasonic treated 70 min	187	3.25	0.294	21.22	2.73

methanol and 0.5 M H_2SO_4 aqueous solutions and normalised to platinum loading are shown in Fig. 6c and Table 2. The peak at around 0.65 V in the forward scan is attributed to methanol oxidation, and the reverse scan peak at around 0.60 V is associated with reaction due to the loss of absorbed intermediates, such as CO_{ads} [52]. Both deposits at room temperature and 0 °C in the absence of CTAB or ultrasonic pretreatment show a very weak peak current, indicating little electrocatalytic activity for methanol oxidation due to fast coalescence of platinum particles or poor adhesion of platinum particles. In contrast, the deposits prepared with CTAB at room temperature and with ultrasonic pretreatment at a 0 °C show the best results. The deposits with CTAB at room temperature show a higher mass activity of 18.36 A g^{-1}, and deposits at 0 °C on ultrasonic pretreated BDD show the highest mass activity for methanol oxidation, 21.22 A g^{-1}, fairly typical for highly dispersed catalysts at this loading [25,53]. The activity in methanol oxidation is also normalised to the platinum surface area measured from hydrogen desorption as surface activity and summarized in Table 2. From this table, the ultrasonic pretreated BDD shows the highest surface activity of 2.73 mA cm^{-2}, much higher than the other three deposition conditions.

The onset potential of methanol oxidation can be used to evaluate the catalyst activity. As shown in Fig. 6c, the lowest onset potential is measured from deposits at 0 °C on ultrasonic pretreated substrate. Although the deposits with CTAB shows quite high mass activity, it exhibits the highest onset potential and oxidation peak potential in the forward scan, probably due to adsorption of surfactant micelles on the catalyst surface that inhibit the methanol oxidation process.

The electrochemical activity of Pt electrocatalysts towards methanol oxidization was investigated further by measuring the anodic polarization curve and calculating kinetic parameters from Tafel plots, as shown in Fig. 6d, which shows data for low Pt loadings. Each plot can be fitted to two linear regions. In the low potential region, the slopes vary from 84.54 to 142.9 mV dec^{-1}, which indicates that the first dehydrogenation of the methanol molecule followed by an electron transfer process is the rate-determining step for methanol oxidation [54,55]. At higher potential, the slope becomes steeper, indicating a change in rate-determining step, likely the removal of intermediates which poison the surface [52]. The Tafel plot also shows that the highest oxidization current at the same potential was achieved for deposition obtained on seeded

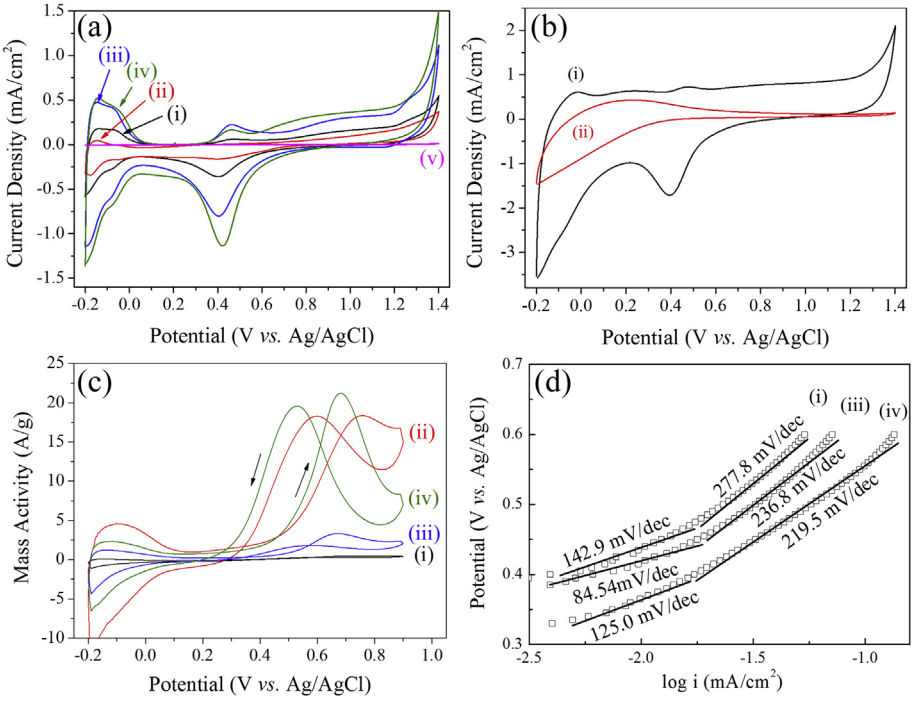

Fig. 6. (a) Cyclic voltammograms of BDD in 0.5 M H_2SO_4 with current normalized to the geometry area of electrode; (b) cyclic voltammograms of glassy in 0.5 M H_2SO_4 with current normalized to the geometry area of electrode, 0 °C in the (i) presence and (ii) absence of an iron wire for 70 min; (c) mass activity in 0.5 M H_2SO_4 and 1.0 M Methanol after normalizing to platinum loading. Deposition conditions are shown in Table 2. (d) Tafel plots of anodic polarization curve for methanol oxidation in 0.5 M H_2SO_4 and 1.0 M Methanol. 10 min deposition times throughout. Deposition conditions using ascorbic acid: (i) at room temperature, (ii) with addition of CTAB at room temperature, (iii) 0 °C, (iv) 0 °C on ultrasonic pretreated BDD, (v) 0 °C in the absence of iron wire for 70 min.

BDD at 0 °C, confirming the best catalytic activity for methanol oxidation from this preparation route.

4. Conclusions

Although at first sight attractive, existing electro- and electroless routes for the deposition of Pt nanoparticles on diamond supports for fuel cell applications are problematic since they lead to very non-uniform deposits (electrodeposition) or require an activating coating (electroless deposition). In the present work we demonstrate a combined process, which involves simultaneous electroless and galvanic processes. The approach solves the uniformity problem associated with electrodeposition on heterogeneous substrates like BDD, and eliminates the requirement of a preactivation process used for conventional electroless deposition.

A range of differing reaction conditions have been explored using differing reducing agents to drive the electroless reaction, reaction temperature, addition of a surfactant and the use of ultrasonic pretreatment. Optimal deposition conditions involve reaction at 0 °C, and the use of ascorbic acid as the reducing agent along with an ultrasonic pretreatment. After optimising the deposition conditions, the Pt deposits are found to exhibit a uniform distribution of particles, and small particle size; they show a high electrochemical activity in terms of a large electroactive area measured from hydrogen desorption, a low onset potential, and a high mass activity and surface activity for methanol oxidisation. The method therefore represents a significant improvement in current electrochemical and electroless approaches for the deposition of Pt nanoparticles on diamond and other inert substrates for electrocatalysis applications.

Acknowledgement

The authors would like to acknowledge the financial support of EPSRC under grant no. EP/F025513/1, and the European Commission Seven Framework Programme – Marie Curie Initial Training Network MATCON (Grant No. FP7-PEOPLE-ITN-2008-238201). Xiao acknowledges scholarship support from China Scholarship Council and Science & Research Project of Education Department of Liaoning Province (Project No. L2012064). Dr Hu acknowledges support from the Ramsay Memorial Fellowships Trust.

References

[1] G. Hoogers, CRC Press, U.S., 2003.
[2] S. Dominguez-Dominguez, J. Arias-Pardilla, A. Berenguer-Murcia, E. Morallon, D. Cazorla-Amoros, J. Appl. Electrochem. 38 (2008) 259–268.
[3] S. Papadimitriou, A. Tegou, E. Pavlidou, S. Armyanov, E. Valova, G. Kokkinidis, S. Sotiropoulos, Electrochim. Acta 53 (2008) 6559–6567.
[4] H. Tang, J.H. Chen, L.H. Nie, D.Y. Liu, W. Deng, Y.F. Kuang, S.Z. Yao, J. Colloid Interf. Sci. 269 (2004) 26–31.
[5] J.J. Wang, G.P. Yin, J. Zhang, Z.B. Wang, Y.Z. Gao, Electrochim. Acta 52 (2007) 7042–7050.
[6] E. Antolini, J. Mater. Sci. 38 (2003) 2995–3005.
[7] H.R. Colon-Mercado, B.N. Popov, J. Power Sources 155 (2006) 253–263.
[8] G. Sine, G. Foti, C. Comninellis, J. Electroanal. Chem. 595 (2006) 115–124.
[9] G. Sine, D. Smida, M. Limat, G. Foti, C. Comninellis, J. Electrochem. Soc. 154 (2007) B170–B174.
[10] G.R. Salazar-Banda, H.B. Suffredini, M.L. Calegaro, S.T. Tanimoto, L.A. Avaca, J. Power Sources 162 (2006) 9–20.
[11] S. Sharma, B.G. Pollet, J. Power Sources 208 (2012) 96–119.
[12] N.R. Stradiotto, K.E. Toghill, L. Xiao, A. Moshar, R.G. Compton, Electroanalysis 21 (2009) 2627–2633.
[13] H.B. Suffredini, V. Tricoli, N. Vatistas, L.A. Avaca, J. Power Sources 158 (2006) 124–128.
[14] X.L. Tong, G.H. Zhao, M.C. Liu, T.C. Cao, L. Liu, P.Q. Li, J. Phys. Chem. C 113 (2009) 13787–13792.
[15] A. Ay, V.M. Swope, G.M. Swain, J. Electrochem. Soc. 155 (2008) B1013–B1022.
[16] D.Y. Kim, B. Merzougui, G.M. Swain, Chem. Mater. 21 (2009) 2705–2713.
[17] L. La-Torre-Riyeros, R. Guzman-Bas, A.E. Mendez-Torres, M. Prelas, D.A. Tryk, C.R. Cabrera, ACS Appl. Mater. Interf. 4 (2012) 1134–1147.
[18] G.R. Salazar-Banda, K.I.B. Eguiluz, L.A. Avaca, Electrochem. Commun. 9 (2007) 59–64.
[19] N. Spataru, X.T. Zhang, T. Spataru, D.A. Tryk, A. Fujishima, J. Electrochem. Soc. 155 (2008) B264–B269.
[20] G.P. Bogatyreva, M.A. Marinich, E.V. Ishchenko, V.L. Gvyazdovskaya, G.A. Bazalii, N.A. Oleinik, Phys. Solid State 46 (2004) 738–741.
[21] Y.Y. Shao, J. Liu, Y. Wang, Y.H. Lin, J. Mater. Chem. 19 (2009) 46–59.
[22] M.C. Granger, M. Witek, J.S. Xu, J. Wang, M. Hupert, A. Hanks, M.D. Koppang, J.E. Butler, G. Lucazeau, M. Mermoux, J.W. Strojek, G.M. Swain, Anal. Chem. 72 (2000) 3793–3804.
[23] R.G. Compton, J.S. Foord, F. Marken, Electroanalysis 15 (2003) 1349–1363.
[24] J. Hu, X. Lu, J.S. Foord, Q. Wang, Phys. Status Solidi A 206 (2009) 2057–2062.
[25] X. Lu, J. Hu, J.S. Foord, Q. Wang, J. Electroanal. Chem. 654 (2011) 38–43.
[26] K.B. Holt, A.J. Bard, Y. Show, G.M. Swain, J. Phys. Chem. B 108 (2004) 15117–15127.
[27] S.H. Wang, G.M. Swain, J. Phys. Chem. C 111 (2007) 3986–3995.
[28] H.V. Patten, K.E. Meadows, L.A. Hutton, J.G. Iacobini, D. Battistel, K. McKelvey, A.W. Colburn, M.E. Newton, J.V. Macpherson, P.R. Unwin, Angew. Chem. Int. Ed. 51 (2012) 7002–7006.
[29] K.D. Beard, J.W.V. Zee, J.R. Monnier, Appl. Catal. B: Environ. 88 (2009) 185–193.
[30] C.R.K. Rao, D.C. Trivedi, Coord. Chem. Rev. 249 (2005) 613–631.
[31] J. Zhao, R. Tian, J. Zhi, Appl. Surf. Sci. 254 (2008) 3282–3287.
[32] C. Ruscior, E. Croiala, J. Electrochem. Soc. 118 (1971) 696–698.
[33] G. Kiss, V.K. Josepovits, K. Kovacs, B. Ostrick, M. Fleischer, H. Meixner, F. Reti, Thin Solid Films 436 (2003) 115–118.
[34] D.F. Cox, G.B. Hoflund, H.A. Laitinen, Langmuir 1 (1985) 269–273.
[35] C.D. Wagner, W.M. Riggs, L.E. Davis, J.F. Moulder, G.E. Muilenburg, Perkin-Elmer Co., 1979.
[36] K. Balakrishnan, J. Schwank, J. Catal. 127 (1991) 287–306.
[37] R. Bouwman, P. Biloen, J. Catal. 48 (1977) 209–216.
[38] M. Aronniemi, J. Sainio, J. Lahtinen, Appl. Surf. Sci. 253 (2007) 9476–9482.
[39] G. Kurbatov, E.D. Ceretti, M. Aucouturier, Surf. Interf. Anal. 20 (1993) 402–406.
[40] J.H. Jang, H.S. Kim, D.P. Norton, V. Craciun, J. Cryst. Growth 311 (2009) 3143–3146.
[41] A.M. Puziy, O.I. Poddubnaya, A.M. Ziatdinov, Appl. Surf. Sci. 252 (2006) 8036–8038.
[42] D. Briggs, M.P. Seah, John Wiley & Sons, Chichester, 1990.
[43] H. Xu, R. Kunz, J.M. Fenton, Electrochem. Solid-State Lett. 10 (2007) B1–B5.
[44] J. Hu, X. Lu, J.S. Foord, Electrochem. Commun. 12 (2010) 676–679.
[45] B. Seger, P.V. Kamat, J. Phys. Chem. C 113 (2009) 7990–7995.
[46] Y.H. Xu, X.Q. Lin, J. Power Sources 170 (2007) 13–19.
[47] F. Montilla, E. Morallon, I. Duo, C. Comninellis, J.L. Vazqueza, Electrochim. Acta 48 (2003) 3891–3897.
[48] A. Esmaeilifar, S. Rowshanzamir, M.H. Eikani, E. Ghazanfari, Electrochim. Acta 56 (2010) 271–277.
[49] K. Sun, J.X. Qiu, J.W. Liu, Y.Q. Miao, J. Mater. Sci. 44 (2009) 754–758.
[50] S.P. Wu, Mater. Lett. 61 (2007) 1125–1129.
[51] S.P. Wu, S.Y. Meng, Mater. Chem. Phys. 89 (2005) 423–427.
[52] J. Zhu, F.Y. Cheng, Z.L. Tao, J. Chen, J. Phys. Chem. C 112 (2008) 6337–6345.
[53] Z.D. Wei, S.H. Chan, J. Electroanal. Chem. 569 (2004) 23–33.
[54] H.A. Gasteiger, N. Markovic, P.N. Ross Jr., E.J. Cairns, J. Electrochem. Soc. 141 (1994) 1795–1803.
[55] A.V. Tripkovic, K.D. Popovic, Electrochim. Acta 41 (1996) 2385–2394.